

pubs.acs.org/chemneuro Research Article

Caged Zn²⁺ Photolysis in Zebrafish Whole Brains Reveals Subsecond Modulation of Dopamine Uptake

Piyanka Hettiarachchi, Sayuri Niyangoda, Austin Shigemoto, Isabel J. Solowiej, Shawn C. Burdette, and Michael A. Johnson*



Cite This: ACS Chem. Neurosci. 2024, 15, 772-782



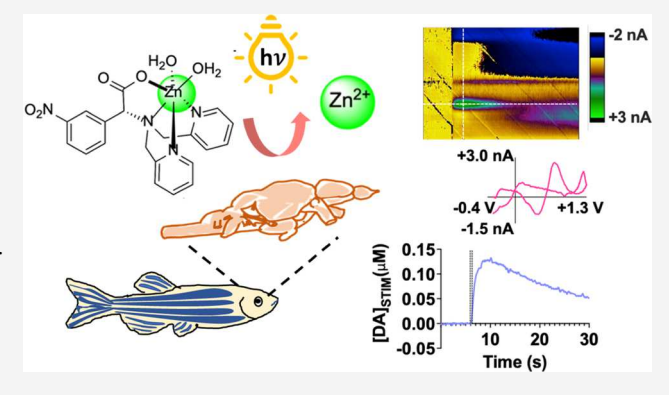
ACCESS I

III Metrics & More

Article Recommendations

s Supporting Information

ABSTRACT: Free, ionic zinc (Zn^{2+}) modulates neurotransmitter dynamics in the brain. However, the sub-s effects of transient concentration changes of Zn^{2+} on neurotransmitter release and uptake are not well understood. To address this lack of knowledge, we have combined the photolysis of the novel caged Zn^{2+} compound $[Zn(DPAdeCageOMe)]^+$ with fast scan cyclic voltammetry (FSCV) at carbon fiber microelectrodes in live, whole brain preparations from zebrafish (*Danio rerio*). After treating the brain with $[Zn(DPAdeCageOMe)]^+$, Zn^{2+} was released by application of light that was gated through a computer-controlled shutter synchronized with the FSCV measurements and delivered through a 1 mm fiber optic cable. We systematically optimized the photocage concentration and light application parameters, including



the total duration and light-to-electrical stimulation delay time. While sub-s Zn^{2+} application with this method inhibited DA reuptake, assessed by the first-order rate constant (k) and half-life $(t_{1/2})$, it had no effect on the electrically stimulated DA overflow $([DA]_{STIM})$. Increasing the photocage concentration and light duration progressively inhibited uptake, with maximal effects occurring at 100 μ M and 800 ms, respectively. Furthermore, uptake was inhibited 200 ms after Zn^{2+} photorelease, but no measurable effect occurred after 800 ms. We expect that application of this method to the zebrafish whole brain and other preparations will help expand the current knowledge of how Zn^{2+} affects neurotransmitter release/uptake in select neurological disease states.

KEYWORDS: zinc, caged compounds, dopamine, zebrafish, voltammetry

■ INTRODUCTION

Zinc is a biogenic transition metal that exists intracellularly and extracellularly in both unbound and bound forms. ^{1,2} It is the second most abundant transition metal in the body, ³ with the brain containing the greatest overall concentration. ⁴ The landmark discovery four decades ago that mossy fiber axons in the hippocampus release and take up free, cationic zinc (Zn²⁺) has spawned a new avenue of research focused on understanding how biogenic transition metals influence neuronal function. ^{5–7} This mobile pool of Zn²⁺, along with other transition metals, is now known to affect how neurons communicate, form memories, and process sensory inputs. ⁸

 Zn^{2+} is presynaptically released from select populations of glutamatergic neurons in the hippocampus, amygdala, striatum, and thalamus, $^{9-11}$ resulting in transiently increased synaptic $(100-300~\mu\text{M})$ and extracellular $(10-20~\mu\text{M})~Zn^{2+}$ levels. 12 Zn^{2+} that is released in the striatum distures to the densely innervating dopaminergic terminals. 13,14 There, it can modulate dopamine (DA) levels through several avenues, including modifying vesicular fusion pore formation 15 and directly inhibiting DA uptake through an allosteric binding site on the DA transporter (DAT). 16 Moreover, released Zn^{2+} alters

neuronal communication by associating with excitatory receptors, including AMPA¹⁷ and NMDA¹⁸ receptors. Zn²⁺ also participates in intracellular signaling pathways; for example, binding to ryanodine receptors increases cytosolic Ca²⁺ transients from the endoplasmic reticulum.¹⁹

Despite these findings, researchers know surprisingly little about the specific effects and underlying mechanisms of action of Zn²⁺ on DA release and reuptake dynamics because the analytical methodology has been underdeveloped. This lack of knowledge is important because in many neurological disorders, homeostatic Zn²⁺ levels may be dysregulated. For example, emerging evidence obtained from Parkinson's disease (PD) model rodents suggests that synaptically released Zn²⁺ may induce behavioral impairment by altering neurotransmission. ¹⁸ Moreover, Zn²⁺ entry into dopaminergic neurons may render

Received: October 16, 2023 Revised: January 13, 2024 Accepted: January 15, 2024 Published: February 1, 2024





them more susceptible to degeneration and dysfunction. ^{19–23} Therefore, it is essential to study how Zn^{2+} influences neuronal function on sub-s time scales, both in health and disease. ^{20,21}

One promising approach to this problem is to use photocaged compounds, which are molecules that, upon exposure to light of sufficient energy and intensity, undergo a structural change that releases a bound substrate, thereby activating a molecule or ion of interest.²² The use of such molecules in biochemistry and physiology is well known and offers a high degree of temporal, spatial, and concentration control through light-initiated reactions.²³ Apart from photocaged small molecules, approaches that employ photocaged divalent metal ions have provided important mechanistic information on signal transduction pathways.^{24–26} For example, Ca²⁺ photocages have been successfully used to elucidate Ca²⁺ signaling,²⁷ ion channel regulation,²⁸ Ca²⁺-dependent vesicle mobilization,²⁹ and muscle contraction³⁰ in both neuronal and non-neuronal cells.^{31–33} However, while physiological and pathophysiological roles of Ca²⁺ ions in various cellular signaling pathways are well established,^{34–36} the similar roles for Zn²⁺ ions are not well characterized.

Several photocleavable (i.e., released by application of light) Zn²⁺ compounds with pronounced photophysical properties and cell permeability have previously been developed.³⁷ These compounds control the bioavailability of Zn2+ until they are exposed to light of a specific wavelength. A line of caged metals, including a photocleavable Zn²⁺ compound known as Zincleav,³⁸ incorporate a chelating backbone and have a quantum yield, defined as moles of molecules that undergo photorelease divided by the moles of photons that have been applied, of about 0.055. 39 Structural refinements have increased the quantum yield to about 0.313.37 To the best of our knowledge, caged zinc compounds are not commercially available. However, commercially available photoactive calcium chelators have quantum yields ranging from about 0.03 to 0.23.22 In this study, we have incorporated a novel, recently developed molecule known as DPAdeCageOMe (2-[bis-(pyridine-2-ylmethyl) amino]-2-(4-methoxy-3-nitrophenyl) acetic acid) to chelate Zn²⁺ and release it upon light application (Figure 1A). The uncaging reaction involves decarboxylation of the cage and a dramatic decrease in its affinity for Zn²⁺.40

Fast scan cyclic voltammetry (FSCV) at carbon fiber microelectrodes is a method of choice for measuring the release/uptake of DA in living brain tissue. ^{41,42} FSCV provides sub-s temporal resolution and good selectivity. ^{41,-46} However, combining FSCV with perfusion or direct injection of free Zn²⁺ through tissues is not an ideal approach for investigating sub-s interactions due to the time needed for Zn²⁺ concentrations to reach equilibrium (minutes to hours). We have previously combined caged compound photolysis with FSCV to quantify glutamate photoactivation in living brain tissue. ⁴⁵ The combination of FSCV with newly developed caged metals, such as caged Zn²⁺ compounds, will allow us to directly probe the effects of free metals on DA release and uptake from presynaptic terminals on sub-s time scales.

In this work, we measured rapid changes in DA release and uptake induced by sub-s application of Zn²⁺. To carry out these measurements, we combined Zn²⁺ photorelease from the recently developed DPAdeCageOMe photocage with FSCV in viable, whole brains from adult zebrafish *ex vivo*. Zebrafish are a valuable research tool because they are easy to alter genetically and are emerging rapidly as an organism to model neurological diseases. ^{46,47} Our results demonstrate that combining FSCV

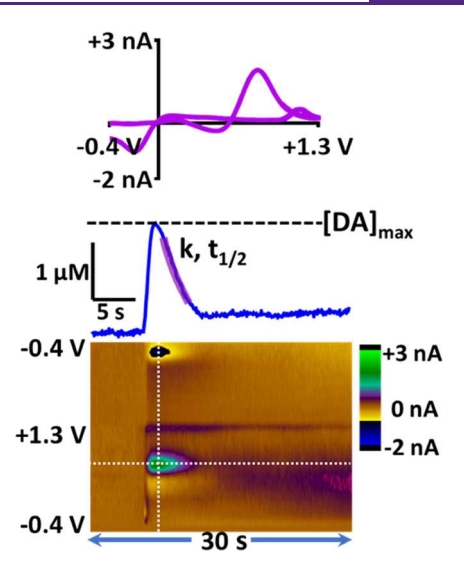


Figure 1. Data were obtained from a typical recording in a zebrafish brain. The stimulated release plot (middle panel) was obtained by sampling the potential indicated by the horizontal dashed line on the color plot (bottom panel). The cyclic voltammogram (top panel) was obtained by sampling at the time indicated by the vertical dashed line and confirms the presence of DA. $[DA]_{MAX}$ concentration was determined by the maximum concentration on the stimulated release plot. The parameters k and $t_{1/2}$, which are used to compare uptake between Zn^{2+} treatments, were obtained by modeling the back portion of the stimulated release plot (purple overlay).

with caged compound photolysis will help unravel the functional relationships between metals and neurotransmitter release/uptake in ways previously unattainable.

RESULTS

Transient Zn2+ Application Affects DA Release and Uptake Differently than Bath Application. Synaptic zinc directly regulates neurotransmitter signaling; hence, Zn²⁺ itself is often referred to as a neurotransmitter. 48 Transient Zn2+ elevations, occurring by neuronal firing, have been linked with various pre- and postsynaptic aspects of neuronal regulation.⁴⁹ Previous studies suggest that Zn^{2+} binds to specific sites on receptors, transporters, and phosphatases. So-52 The specific mechanisms of actions of Zn^{2+} on neurotransmitter regulation are highly complex and have not yet been fully explored. To help elucidate these mechanisms, we have applied FSCV to intact, viable zebrafish brains. We have analyzed data obtained from each recording to determine the peak dopamine overflow ([DA]_{MAX}). We further analyzed these data by modeling the curves to determine the first-order rate constant of DA uptake (k) and the half-life of DA uptake $(t_{1/2})$. This operation is illustrated in Figure 1. Shown in Figure 2 are results from a 60 min bath application of Zn²⁺ to the zebrafish whole brain. We note from control measurements that any oxidation or reduction currents from Zn²⁺ did not interfere with the ability to measure DA release and uptake (Figure S1). The peak current arising from the DA overflow (Figure 2A) roughly doubled after addition of 100 μ M Zn²⁺. Additionally, modeling the back side of the stimulated release plot revealed a sharp decrease in k and increase in $t_{1/2}$. Given previous findings that an allosteric $\mathrm{Zn^{2+}}$ binding site is present on human DAT, ^{53,54} an inhibition of DA uptake is expected. However, it is unclear if the enhancement of the peak current results from an increase in DA release or solely from inhibition of DA uptake. Additionally, the cellular

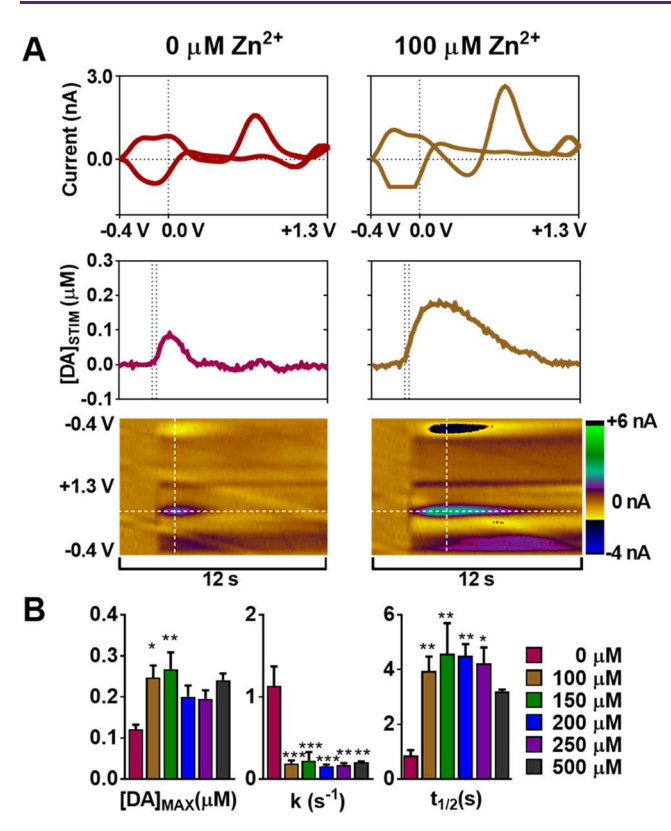


Figure 2. Addition of Zn2+ to aCSF significantly affects evoked dopamine release and uptake. (A) Representative plots of stimulated dopamine release and uptake before and after Zn²⁺ was administered in aCSF to the same brain with the electrode positioned at a single location. The vertical dotted lines on the stimulated release plots indicate the initiation and duration of the electrical stimulus. The horizontal dashed lines on the respective color plots indicate the potential at which the current was sampled to obtain the release plots. The vertical dashed lines indicate the time at which the CVs (top panels) were sampled to indicate the presence of dopamine. The red traces represent $0 \mu M Zn^{2+}$ added, and the brown traces represent 100 μ M Zn²⁺ added. (B) Bar graphs of [DA]_{MAX}, k, and $t_{1/2}$. Within group effects (one-way ANOVA), [DA]_{MAX}, p = 0.0088, k, p = 0.0013, $t_{1/2}$, p =0.0001, N = 3-5 fish. Tukey post hoc, *p < 0.05, **p < 0.01, ***p < 0.01 $0.005 \text{ vs } 0 \mu\text{M}.$

mechanisms responsible for this sharp increase in the dopamine overflow are not known. Therefore, to assess the effect of Zn²⁺ signaling on uptake more accurately, it is necessary to use an approach that allows collection of these measurements without allowing possible changes in release that occur over long time periods.

To accomplish this goal, we combined the Zn²⁺ photorelease with FSCV. A description of the photorelease reaction and experimental setup is provided in Figure 3. This newly developed approach of applying biologically active metal ions enables us to capture the effects of transient zinc application on DA release and clearance in zebrafish whole brains directly. In a representative recording session, we set up the flow so that a zebrafish brain was superfused with aCSF having 100 μ M [Zn(DPAdeCageOMe)]⁺. To photouncage Zn²⁺, we applied a 1000 ms light pulse, ending 500 ms prior to electrical stimulation. Figure 4A shows representative DA release plots obtained prior to adding [Zn(DPAeCageOMe)]+ ("naive"), prior to adding [Zn(DPAeCageOMe)] but after applying light ("light"), after adding [Zn(DPAeCageOMe)]+ ("caged Zn²⁺"), and after adding [Zn(DPAeCageOMe)]⁺ and applying light

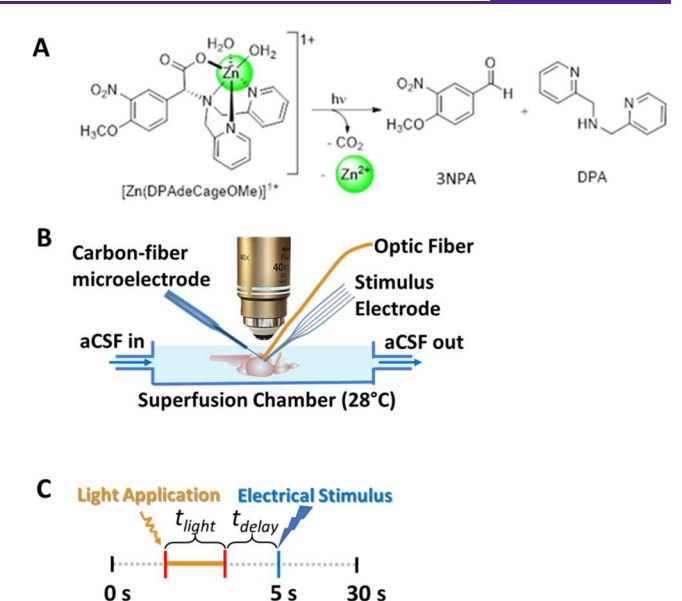


Figure 3. Description of photouncaging measurements. (A) Photouncaging reaction of [Zn(DPAdeCageOMe)]+. (B) Micropositioning of the electrical stimulus electrode, 1 mm optic fiber, and carbon fiber microelectrode in the telencephalon region of the zebrafish brain (not to scale). (C) Timeline for the photouncaging events. The total time of the FSCV data collection was 30 s. In this example, the light pulse was applied at 1.5 s with 2 s exposure time duration (t_{light}) and the electrical stimulation was applied 5 s after the light for a stimulus delay time $(t_{\rm delay})$ of 1.5 s. Note: The values of $t_{\rm light}$ and $t_{\rm delay}$ in panel (C) were selected for illustrative purposes. The actual experimental values of $t_{\rm light}$ and $t_{\rm delay}$ were of a smaller magnitude.

30 s

5 s

("uncaged"). DA release was not significantly altered by any of these events (p = 0.5820, main effect, one-way ANOVA, n = 4brains) (Figure 4B). However, modeling the DA release curves revealed that DA reuptake was slowed by the photouncaging of the [Zn(DPAdeCageOMe)] + complex. The pooled data, shown in Figure 4C,D, further confirm this observation. Analysis with one-way ANOVA indicated that the DA reuptake rate constant (k) significantly decreased after photouncaging of the [Zn-(DPAdeCageOMe)]⁺ complex (p < 0.0001, main effect, n = 4brains). Furthermore, Dunnett's multiple comparison test revealed significant differences between the mean value of k after photouncaging and naïve, light-treated, and caged Zn2+ mean values of k (p = 0.0003, uncaged vs light-treated; p <0.0001, uncaged vs naive; p = 0.0003, uncaged vs caged Zn^{2+} ; n =4 brains). The half-life of DA $(t_{1/2})$ followed a similar trend (p =0.0007, main effect, one-way ANOVA; p = 0.016, uncaged vs light-treated; p = 0.0035, uncaged vs naive; p = 0.0045, uncaged vs caged Zn^{2+} ; Dunnett's multiple comparison test, n = 4 brains). Additional control measurements, in which we exposed brains to light from our system and treated brains with the photouncaging byproducts 3NPA and DPA (see Figure 4A), revealed no effect on $[DA]_{MAX}$, k, or $t_{1/2}$ (Figures S2 and S3) and no effect was apparent after washing out the photocaged Zn²⁺ for 30 min (Figure S4). Thus, our results indicate that photorelease of Zn²⁺ immediately (<1 s) impaired DA uptake, while the addition of the drug without light and the application of light without the drug had no effect on performance or viability (Figure 4B).

Effect of Caged Compound Concentration on DA Release and Uptake. Here, we determined how the [Zn(DPAdeCageOMe)]⁺ concentration affects dopamine release and uptake. The concentration of [Zn-

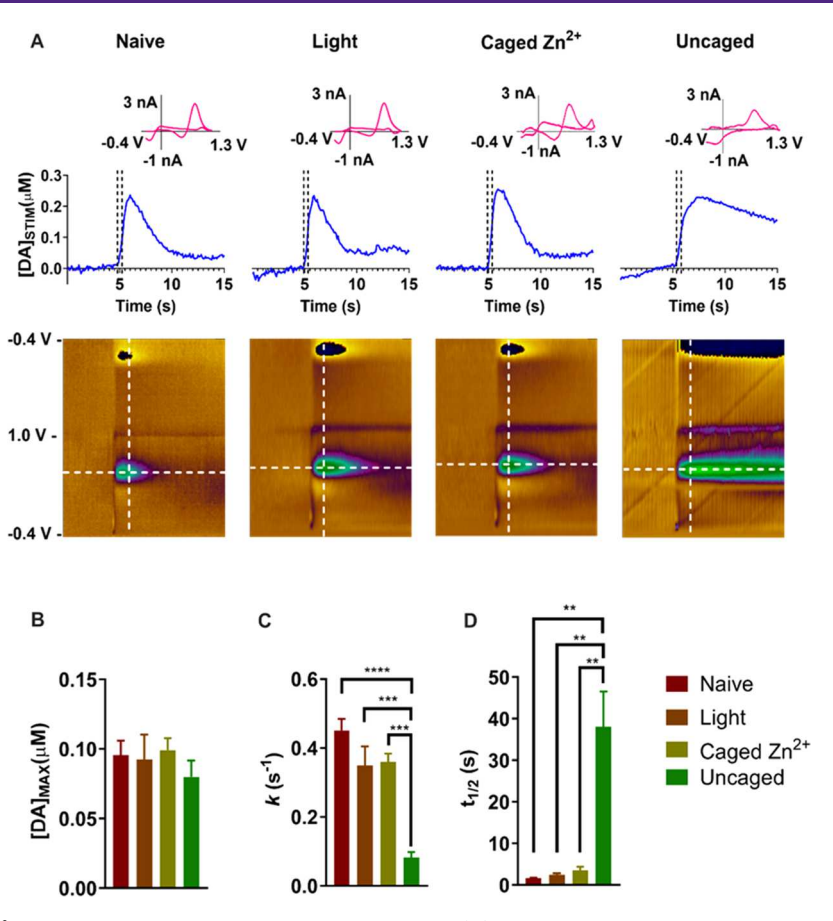


Figure 4. Photouncaged Zn²⁺ decreases DA uptake in live zebrafish brains. (A) Representative color plots, stimulated release plots and cyclic voltammograms. The stimulus consisted of 15 biphasic pulses, 2 ms duration/pulse, 350 μA, and 60 pulses/s. The stimulus duration is indicated by the vertical dashed lines. The main effects determined using one-way ANOVA (n = 4 brains) are (B) released DA concentration (p = 0.5820); (C) DA reuptake rate constant (k) (p = 0.0001); and (D) half-life of DA uptake ($t_{1/2}$) (p = 0.0032). **p < 0.01, ***p < 0.001, and ****p < 0.0001, Dunnett's multiple comparison test. The values of t_{delay} and t_{light} were 500 and 1000 ms, respectively.

(DPAdeCageOMe)]⁺ was changed (50–150 μ M) (500 ms) constantly.

The results, shown in Figure 5, indicate that $[DA]_{MAX}$ did not change, compared to the naïve value, with increasing $[Zn-(DPAdeCageOMe)]^+$ concentration up to 150 μ M (p=0.7331, main effect, one-way ANOVA). However, k (p=0.0244, main effect, one-way ANOVA) and $t_{1/2}$ (p=0.0203, main effect, one-way ANOVA) were sensitive to the $[Zn(DPAdeCageOMe)]^+$ concentration.

Dunnett's multiple comparison post hoc analysis revealed that 100 and 150 μ M concentrations had a significant effect on k (p =0.0460,100 μ M; p = 0.0202, 150 μ M) and $t_{1/2}$ (p = 0.0379, 100 μ M; p = 0.0273, 150 μ M), while 50 μ M had no significant effect $(p = 0.6884 \text{ for } k, p = 0.8971 \text{ for } t_{1/2})$. The likely reason for this disparity is that photolysis of [Zn(DPAdeCageOMe)]+ at a concentration of 50 µM produces Zn2+ at insufficient concentration to exert a measurable effect on DA clearance. The effect appeared to peak at 100 μ M; therefore, we used this concentration for the other photouncaging measurements. Without the development of additional analytical methodology, it is not possible to know precise concentrations of Zn² photoreleased in the opaque brain environment since we cannot accurately quantify light reaching the spot of measurement. However, the photolysis of 100 μ M [Zn(DPAdeCageOMe)]⁺ likely provides Zn2+ concentrations in line with naturally occurring transient extracellular (10–20 μ M) Zn²⁺ levels, given that the quantum yield is $\sim 30\%^{37}$ and that light of decreased intensity would penetrate the opaque environment of the brain.

Increasing the Light Exposure Time Decreases the DA **Uptake Rate.** We also examined the effect of t_{light} in the presence of the [Zn(DPAdeCageOMe)]+ complex on DA release and uptake. Recordings were collected at exposure times that ranged from 0 to 1000 ms. Figure 6A shows the representative, color plots, DA release plots, and cyclic voltammograms before the application of [Zn-(DPAeCageOMe)]+ or light ("naive") and three different light pulse durations (200, 600, and 1000 ms). Pooled data from multiple brains are shown in Figure 6B-D. Increases in light exposure time dramatically impaired DA clearance, given that k decreased (p = 0.0037, main effect, one-way ANOVA, n = 7brains) (Figure 6C) and half-life $(t_{1/2})$ increased (p = 0.0019,main effect, one-way ANOVA, n = 7 brains) (Figure 6D). Dunnett's multiple comparison post hoc test revealed no difference in k or $t_{1/2}$ at 0–200 ms. However, exposure to light at durations of 400-1000 ms significantly decreased k (p =0.0213, 400 ms; p = 0.0174, 600 ms; p = 0.0052, 800 ms; p = 0.00520.0044, 1000 ms), while exposure at durations of 600-1000 mssignificantly increased $t_{1/2}$ (p = 0.0343, 600 ms; p = 0.0047, 800 msms; p = 0.0050, 1000 ms).

These data indicate that increasing Zn^{2+} release by photouncaging of the $[Zn(DPAdeCageOMe)]^+$ complex progressively decreases uptake. In our system, light applied at brief durations (0–200 ms) did not result in a change of k and $t_{1/2}$,

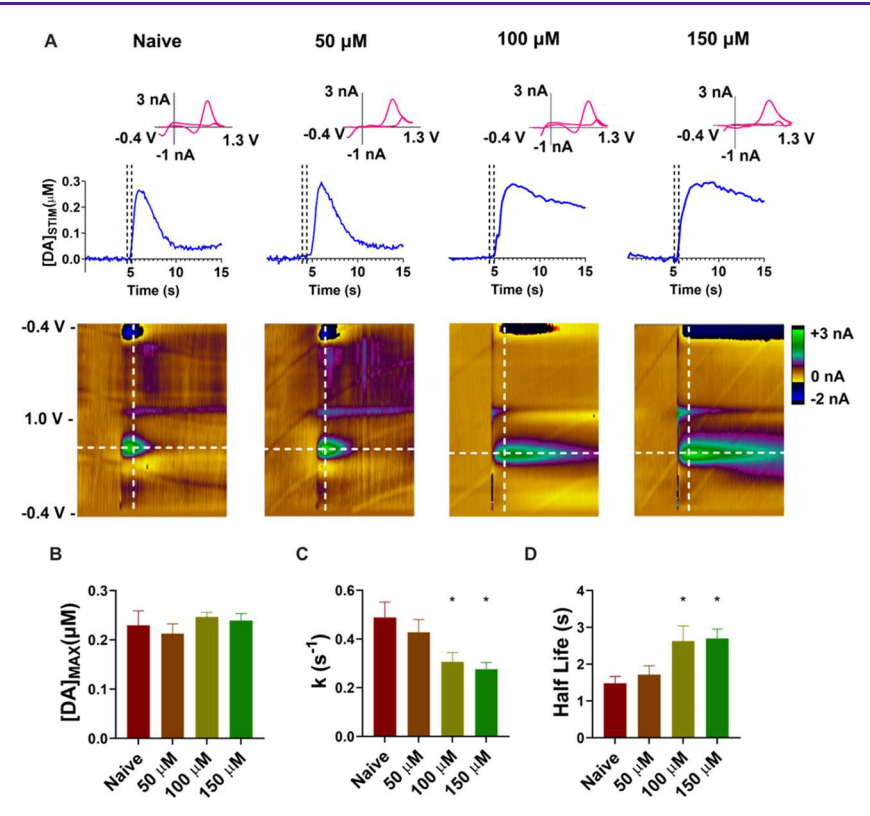


Figure 5. Increasing the caged compound concentration decreases the level of DA uptake but has no effect on DA release. (A) Representative color plots, stimulated release plots, and cyclic voltammograms. The main effects determined using one-way ANOVA (n = 4 brains) are (B) released DA concentration (p = 0.7331); (C) k (p = 0.0244); and (D) $t_{1/2}$ (p = 0.0203). *p < 0.05, Dunnett's multiple comparison test. The values of t_{delay} and t_{light} were 500 and 1000 ms, respectively.

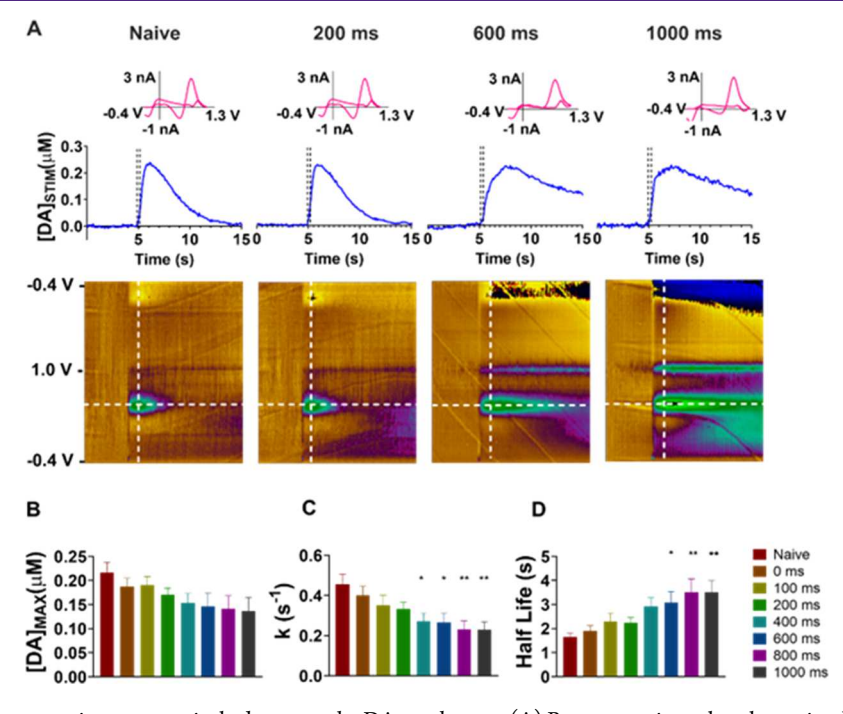


Figure 6. Increasing light exposure time progressively decreases the DA uptake rate. (A) Representative color plots, stimulated release plots, and cyclic voltammograms for DA relase from naive brains and from brains treated with $t_{\rm light}$ times of 200, 600, and 1000 ms. The main effects determined using one-way ANOVA (n = 7 brains) are (B) released DA concentration (p = 0.1535); (C) k (p = 0.0037); and (D) $t_{1/2}$ (p = 0.0019). *p < 0.05, **p < 0.01, Dunnett's multiple comparison test. The value of $t_{\rm delay}$ was 500 ms, and the concentration of [Zn(DPAeCageOMe)]* was 100 μM.

while light applied at greater durations (>200 ms) did. These longer durations, therefore, are necessary to provide a concentration of Zn^{2+} that can inhibit uptake. Critically, our

results also indicate that we can control the bioavailability of Zn^{2+} by controlling the light exposure time duration.

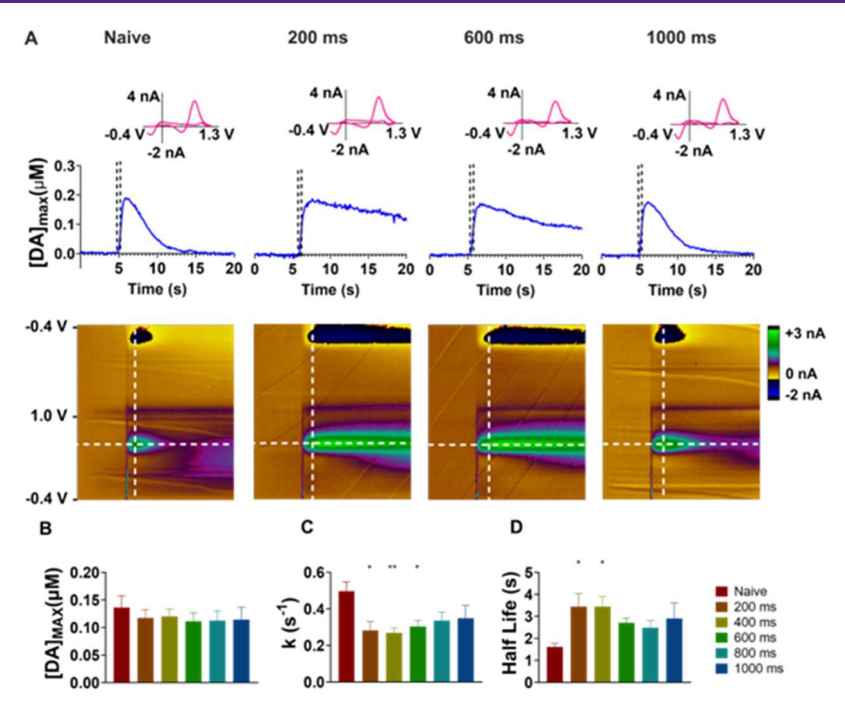


Figure 7. Shorter delay times enhance the effects of Zn^{2+} photorelease. (A) Representative color plots, stimulated release plots, and cyclic voltammograms for DA relase with naïve, 200, 600, and 1000 ms light to electrical stimulation delay times. Main effects from one-way ANOVA (n = 7 brains) are as follows: (B) released DA concentration (p = 0.9321); (C) k (p = 0.0224); (D) $t_{1/2}$ of DA (p = 0.0661). *p < 0.05, **p < 0.01, Dunnett's multiple comparison test. The value of t_{light} was 500 ms, and the concentration of [Zn(DPAeCageOMe)]⁺ was 100 μ M.

Shorter Stimulation Delay Times Correspond to a **Greater Effect on DA Uptake.** As shown in Figure 3C, there is a time gap between the end of the light application time and the start of the electrical stimulation of DA release (t_{delay}) . Optimization of t_{delay} is important because it is the time needed for uncaged Zn²⁺ to influence DA uptake. In this experiment, we systematically increased $t_{\rm delay}$ from 200 to 1000 ms while keeping the light exposure time (1000 ms) and the electrical stimulation parameters constant (15 pulses, 60 Hz, 2 ms, 350 μ A). Figure 7A depicts representative DA release plots and cyclic voltammograms obtained ex vivo in brains prior to light application (naive) and after light was applied at a t_{delay} of 200, 600, and 1000 ms. Figure 7B shows the pooled data for $[DA]_{MAX}$, k, and $t_{1/2}$. Like the previous measurements in Figures 4-6, [DA]_{MAX} did not significantly change (p = 0.9321, main effect, one-way ANOVA, n = 7 brains), while delay times of 200–600 ms had a significant effect on k (p = 0.0224, main effect, one-way ANOVA, n = 7brains). The results of Dunnett's multiple comparison post hoc analysis revealed that *k* values at the 200, 400, and 600 ms delay times were different from the naive k values (p = 0.0133, 200 ms; p = 0.0077, 400 ms; p = 0.0294, 600 ms). The overall main effect of t_{delay} on $t_{1/2}$ was not statistically significant (p = 0.0661, main effect, one-way ANOVA, n = 7 brains). However, the results of Dunnett's multiple comparison post hoc analysis revealed that $t_{1/2}$ values at the 200 and 400 ms delay times were significantly different from the respective naive $t_{1/2}$ values (p = 0.0296, 200ms; p = 0.0289, 400 ms).

DISCUSSION

In this study, we have developed a method that combines caged $\mathrm{Zn^{2+}}$ photorelease with FSCV and have used this approach to examine how sub-s $\mathrm{Zn^{2+}}$ application influences the stimulated release and uptake of DA in whole zebrafish brains. Although DA release appeared to be unaffected, uptake was diminished. In contrast, a 1 h bath application of brains in $\mathrm{Zn^{2+}}$ -containing

sCSF appeared to increase both DA release and uptake. After optimizing the concentration of the $[Zn(DPAdeCageOMe)]^+$ complex, we further showed that increasing the light exposure time enhances the effect of Zn^{2+} photorelease on uptake. Moreover, the degree of uptake inhibition by Zn^{2+} decreased with an increased delay time between light application and electrical stimulation.

Previous studies have identified Zn^{2+} as an endogenous allosteric modulator of the DAT, 16,53 which terminates synaptic dopaminergic neurotransmission by reuptake of extracellular DA into the presynaptic neurons. The binding site of Zn^{2+} on DAT consists of four amino acid residues and is located on the extracellular part of the protein. S5,56 Several studies have suggested that binding Zn^{2+} inhibits the action of DAT likely by the hindrance of a conformational change essential for the transport process. Therefore, the slow DA clearance rate that we observed with the photouncaging of the [Zn-(DPAdeCageOMe)]+ complex and bath application with Zn^{2+} is likely due to the inhibition of DAT through Zn^{2+} binding to this site.

Another interesting aspect of these findings is that a 1 h bath application of brains in $Zn^{2+}\text{-containing}$ aCSF induced a significant increase in $[DA]_{MAX}$, while sub-s photorelease of Zn^{2+} appeared to have no effect. Although it is difficult to pinpoint a specific mechanism underlying this phenomenon, it is likely that the amount of time during which brains were exposed to Zn^{2+} is important. On sub-s time scales, Zn^{2+} binds to extracellular targets and can influence release rapidly. For example, Zn^{2+} binding to sites on D1- and D2-type DA receptors results in altered binding kinetics of DA. 59,60

D2 DA autoreceptors are located presynaptically on dopamine terminals in mammalian and teleost brains and serve as a feedback mechanism through several actions. Activation results in the rapid inhibition of DA release probability by inhibition of voltage-gated calcium channels

(P/Q and N-type), 61,62 membrane hyperpolarization through activation of voltage-dependent potassium channels $(K_V1.2)$, 63,64 and enhancement of DA uptake by association with dopamine transporter molecules. $^{65-70}$ This fast inhibition of release can occur within hundreds of milliseconds. 65,71 Additionally, D2 autoreceptor activation results in the inhibition of DA synthesis, which occurs over a longer period of time. 72,73

Our previous studies have shown that pharmocological inhibition of D2 and D3 autoreceptors increases DA release in this zebrafish brain preparation. The other hand, postsynaptic D1 and D2 receptors may also impact release in this whole brain preparation, given that the circuitry is intact. It is unclear how quickly autoreceptor activation alters DA release in zebrafish; therefore, we cannot exclude the possibility that the disruption of binding of DA to D2 receptors by Zn²+ has influenced DA release in our preparation. Nevertheless, our findings suggest that sub-s Zn²+ photorelease primarily affects DA uptake.

Over longer periods of time, Zn²⁺ may enter cells and affect other targets. For example, it binds to Src kinase, which upregulates NMDA receptors⁷⁵ and activates TrkB receptors.⁷⁶ Additionally, Zn²⁺ binds to metal regulatory transcription factor-1 (MTF-1), upregulating transcription of various gene targets associated with maintaining zinc homeostasis, including metallothionein-2 (MT-2), metallothionein-3 (MT-3), and zinc transporter-1 (ZnT1).^{77,78} Intracellular Zn²⁺ can also influence the regulation and function of multiple membrane receptors, including upregulating M-type potassium channels.⁷⁹ In our study, these and other mechanisms may have influenced DA release and uptake following the 1 h-duration bath application of brains in Zn²⁺. Given that intracellular Zn²⁺ plays numerous signaling roles, it is difficult and beyond the scope of this work to identify which mechanisms may increase the DA overflow after a 1 h-long exposure to Zn²⁺; however, the roles that intracellular Zn²⁺ plays in DA release should be examined in the future. Collectively, the results of these measurements support the feasibility of our approach of using photocaged compound photolysis combined with FSCV measurements to study the regulation of neurotransmitter release and uptake by metal ions.

We also found that as we increased $t_{\rm delay}$, uptake tended to return to normal. This finding may be explained by the rapid diffusion of ${\rm Zn^{2+}}$ immediately after its photorelease. The diffusion of the ions in the brain extracellular space is complex and is constrained by several factors, such as volume fraction and tortuosity. Syková and Nicholson have studied the diffusion of molecules in the brain and developed a modified diffusion equation to analyze the transport behavior of several molecules. Furthermore, a recent study combined theoretical and experimental approaches to study the diffusion of ${\rm Zn^{2+}}$ in the synaptic cleft. Their findings suggest that the ${\rm Zn^{2+}}$ concentration exponentially decreases over 100 ms. Our results indicate that ${\rm Zn^{2+}}$ had diffused sufficiently so that there was no effect on uptake after 800 ms.

Furthermore, zinc transporters (ZnTs) and metallothionines (MTs) are known to regulate zinc homeostasis in the cellular and subcellular environment. MTs serve as buffers against rising Zn²⁺ levels in the intracellular environment. They maintain homeostasis by trapping free cytosolic Zn²⁺. ZnTs help regulate overall zinc balance and distribution within cells. Previous studies revealed that increased zinc exposure elevated the functions and expression of MTs and ZnTs. Rence, the diminishing effects on k and $t_{1/2}$ at greater $t_{\rm delay}$ values might arise

from the combined functions of MTs, ZnTs, and extracellular diffusion

A consensus is coalescing around the idea that altered homeostatic levels of Zn2+ play a significant role in many neurological disorders. These disorders (reviewed by Wang et al. 84) include neurodegenerative conditions such as Alzheimer's disease (AD), Parkinson's disease (PD), and multiple sclerosis (MS); psychiatric disorders such as depression and schizophrenia; epilepsy; and traumatic brain injury. In the case of neurodegenerative disorders, especially PD, it is important to understand how DA regulation is altered. Oxidative stress is known to play an important role in PD and Zn²⁺ binds to DAT in part by its association with histidine residues, 53,54 which are particularly vulnerable to covalent modifications caused by reactive oxygen species.⁸⁵ These modifications likely decrease the ability of Zn²⁺ to bind to this site. Our approach of combining FSCV with caged Zn²⁺ photorelease can be used in combination with mass spectrometric techniques to assess the effects of these modifications on DAT performance.

Our approach can also be used to resolve neurochemical mechanisms that underlie depression. For example, serotonin signaling has long been implicated in depression, and chronic administrations of SSRIs, such as escitalopram and fluoxetine, are front-line treatments that enhance serotonin levels. However, little attention has been given to how Zn²⁺ interacts with 5-H1A receptors, which can function as autoreceptors on presynaptic terminals, thereby regulating serotonin release. Like DAT, the function of this receptor type is inhibited by Zn²⁺ associating with it via an allosteric binding site. Heasurement of serotonin release and uptake with FSCV, combined with caged compound photorelease, promises to reveal how the subsfunction may be altered under conditions that cause depression, in both zebrafish and rodent models.

CONCLUSIONS

In this study, we combined Zn caged compound photolysis with FSCV to determine how transient Zn2+ release influences DA release/reuptake in whole zebrafish brains ex vivo. We found that the photorelease of Zn^{2+} from the $[Zn(DPAdeCageOMe)]^{+}$ complex decreases DA uptake, with greater light exposure times and smaller delay times increasing this effect. Together, these results demonstrate that caged compound photolysis combined with FSCV can be used to investigate the effects of transient metal ion fluctuations on neurotransmitter dynamics with controlled spatial and temporal resolution. Moreover, dysregulation of zinc homeostasis is associated with the pathogenesis of multiple neurological conditions, including Alzheimer's disease, ⁸⁸ Parkinson's disease, ⁸⁹ amyotrophic lateral sclerosis, ⁹⁰ traumatic brain injury, ⁹¹ depression, ⁹² and schizophrenia. ⁹³ Thus, the ability to control the spatial and temporal availability of Zn²⁺ ions afforded by our new method could be particularly beneficial in understanding the role of Zn²⁺ under these conditions.

METHODS

Chemicals. The Zn²⁺ caged compound, DPAeCageOMe (2-[bis(pyridine-2-ylmethyl) amino]-2-(4-methoxy-3-nitrophenyl) acetic acid), was synthesized as previously described. For [Zn-(DPAeCageOMe)]⁺ preparation, DPAeCageOMe was dissolved in zinc-free artificial cerebrospinal fluid (aCSF; 126 mM NaCl, 2.5 mM KCl, 2.4 mM CaCl₂, 1.2 mM MgSO₄, 25 mM NaHCO₃, 1.2 mM MgCl₂ and 20 mM HEPES, adjusted to a pH of 7.4) to give a final concentration of 100 μ M. For the concentration study described in

Figure 5, aCSF containing 50, 100, and 150 μ M DPAeCageOMe was made. ZnCl₂ (lot no.: MKCN6765, 98%, Sigma-Aldrich, St. Louis, MO) and DPAeCageOMe solutions were mixed in 1:1 molar ratio to prepare [Zn(DPAeCageOMe)]⁺ of the desired concentration. Standards for the uncaging byproducts, 4-methoxy-3-nitrobenzaldehyde (3NPA; lot number MKBR4377V) and di-(2-picolyl)amine (DPA; lot number MKCP3723), were obtained from Sigma (St. Louis, MO).

Animals. The University of Kansas Institutional Animal Care and Use Committee approved all animal procedures. Wild-type adult *Danio rerio* (zebrafish, AB wild-type strain) were bred and housed at the University of Kansas. Fish were maintained in a tank system as previously described. ⁴⁵ Water quality was monitored, and parameters were maintained: conductivity, $800 \, \mu \text{S cm}^{-1}$; pH, 7.2; and temperature, $28\,^{\circ}\text{C}$. A light/dark cycle of 14 h on and 10 h off was used. Fish received food twice daily.

Zebrafish Brain Preparation. After euthanasia by rapid chilling and decapitation, the head was mounted on a 2% agarose Petri dish submersed in ice-cold, oxygenated aCSF. The skull was dissected under a stereoscope and the brain was placed in a heated (28 °C) superfusion chamber. The superfusate consisted of aCSF maintained at 28 °C and saturated with oxygen/carbon dioxide (95%/5%). The zebrafish aCSF composition was modified for each zinc photorelease recording session to prevent zinc precipitation and consisted of 131 mM NaCl, 2 mM KCl, 20 mM NaHCO₃, 2 mM MgCl₂, 10 mM glucose, 2.5 mM CaCl₂· H₂O, and 10 mM HEPES dissolved in purified (18.2 MΩ) water (pH 7.35–7.4). The brain was anchored in place with a nylon mesh harp (Warner Instruments, Holliston, MA).

Fast Scan Cyclic Voltammetry. Cylindrical carbon fiber microelectrodes (CFMEs) were fabricated using previously published procedures. 95 Briefly, glass barrels (1.2 mm D.D. and 0.68 mm LD, 4 in. long; A-M Systems Inc., Carlsberg, WA) were loaded by suction with single carbon fibers (7 µm diameter, Goodfellow Cambridge LTD, Huntingdon, U.K.). Loaded barrels were heated and pulled with a PE-22 heated coil puller (Narishige Int. USA, East Meadow, NY). Exposed carbon fiber tips were cut to 100 μm from the glass seal. EPON resin 815C and EPIKURE 3234 curing agent (Miller-Stephenson, Danbury, CT) were used to seal each electrode. Electrodes were dipped for 30 s into the resin, dipped into toluene, and cured at 100 °C for at least 1 h. Measurements were obtained with an integrated system that consisted of a Dagan Chem-Clamp potentiostat (Dagan, Minneapolis, MN), a personal computer with National Instruments computer interface cards (PCI 6052 and PCI 6711, National Instruments, Austin, TX), and a breakout box. Tar Heel CV software (provided by R.M. Wightman, University of North Carolina, Chapel Hill, NC) was used to collect measurements. For measurements in brains, the applied waveform parameters were as follows: scan rate, 400 V/s; waveform application frequency, 10 Hz; and waveform potentials applied, -0.4 to +1.3 V to -0.4 V (vs Ag/AgCl reference electrode). Prior to obtaining measurements, the carbon fiber surface was pretreated by applying the waveform at an application frequency of 60 Hz for 15 min, followed by 10 Hz for 10 min. Release was evoked by the coordinated application of multiple biphasic stimulus pulses (15 pulses, 60 Hz, 2 ms, 350 μ A). These pulses were applied to two tungsten electrodes positioned 200 μ m apart. The carbon fiber working electrode was positioned in the dorsal nucleus of the ventral telencephalon (V_d) between the two stimulation electrodes, a spot in the brain that is innervated with dopaminergic fibers that originate in the posterior tubercle (PT). We have previously carried out pharmacological studies in which the norepinephrine transporter was inhibited to ensure that norepinephrine release did not contribute to the electrochemical signal. 41,74 Brains were given 10 min recovery time between electrical stimulations.

Photouncaging of [Zn(DPAeCageOMe)]*. An overview of a typical recording session with a more detailed description is shown in Figure 1B,C. The brain was perfused with [Zn(DPAeCageOMe)]* in oxygenated aCSF that was recycled with a peristaltic pump. An optical fiber (1 mm diameter) was positioned above the telencephalon region of the brain, close to the carbon fiber microelectrode. A single light pulse, supplied by a mercury lamp, was applied by transient opening of a shutter (LS6ZM2, Uniblitz electronics, Rochester, NY) activated by a custom controller designed by the University of Kansas Instrument

Design Laboratory (KU-IDL). This controller was operated by software written by the KU-IDL and activated by a + 5 V transistortransistor logic (TTL) signal received from Tar Heel software. This arrangement provided synchronicity between light pulses and electrical stimuli. Light from the mercury lamp was supplied by a fiber optic cable (PolyMicro Technologies, Inc., Phoenix, AZ). After a set delay period after the TTL signal application, specified in Tar Heel software, the electrical stimulus pulse(s) was applied, and the released amount of DA was measured with FSCV. For method optimization and rigor, light toxicity for the DA measurements was measured by applying light pulses up to 1000 ms without the application of the caged compound. To determine optimum light exposure time, DA release and uptake measurements were taken while adjusting the light exposure duration (t_{light}) at values ranging from 0 to 1000 ms. Next, the optimal delay time between light application and electrical stimulation (t_{delay}) was determined by collecting recordings at values ranging from 0 to 1000 ms. The effect of the caged compound concentration was measured by changing the concentration while keeping $t_{\rm light}$ and $t_{\rm delay}$ constant.

Data Analysis and Statistics. GraphPad Prism 7 (GraphPad Software, Inc., La Jolla, CA) was used for statistical analysis and graphing. For all of the listed experiments, the reported data are presented as a mean value \pm the standard error of the mean (SEM). The N value listed for all of the experiments indicates the number of whole fish brains used. Figure 1D illustrates the data obtained from each stimulated release plot. To determine the peak DA overflow ([DA]_{MAX}), the maximum current for DA release (i_{MAX}) was determined by using Tar Heel software. $[\mathrm{DA}]_{\mathrm{MAX}}$ was then determined by comparing this current with values obtained by calibrating the electrode against DA standard solutions in a flow cell. The modeling of stimulated release plots was performed with GraphPad software specifically to compare DA uptake in zebrafish brains before and after Zn²⁺ photorelease occurred. DA uptake was then modeled in GraphPad to determine k, the first order rate constant of uptake, and $t_{1/2}$, the halflife of uptake. We used these results to determine how k and $t_{1/2}$ changed in a given brain over time. DA reuptake by DAT was determined using the nonlinear regression plateau followed by one phase decay model of GraphPad, as we have previously published.⁷

ASSOCIATED CONTENT

Supporting Information

The Supporting Information is available free of charge at https://pubs.acs.org/doi/10.1021/acschemneuro.3c00668.

Presence of Zn²⁺ not affecting the ability to measure dopamine with FSCV, light and exposure to photouncaging byproducts not significantly influencing dopamine release and uptake, and 30 min washout experiment confirming the absence of residual effects (PDF)

AUTHOR INFORMATION

Corresponding Author

Michael A. Johnson – Department of Chemistry and R. N. Adams Institute for Bioanalytical Chemistry, University of Kansas, Lawrence, Kansas 66045, United States;

orcid.org/0000-0001-5078-9896; Phone: 785-864-4269; Email: johnsonm@ku.edu

Authors

Piyanka Hettiarachchi — Department of Chemistry and R. N. Adams Institute for Bioanalytical Chemistry, University of Kansas, Lawrence, Kansas 66045, United States

Sayuri Niyangoda – Department of Chemistry and R. N. Adams Institute for Bioanalytical Chemistry, University of Kansas, Lawrence, Kansas 66045, United States

Austin Shigemoto – Department of Chemistry and Biochemistry, Worcester Polytechnic Institute, Worcester, Massachusetts 01609, United States

- **Isabel J. Solowiej** Department of Chemistry and R. N. Adams Institute for Bioanalytical Chemistry, University of Kansas, Lawrence, Kansas 66045, United States
- Shawn C. Burdette Department of Chemistry and Biochemistry, Worcester Polytechnic Institute, Worcester, Massachusetts 01609, United States; orcid.org/0000-0002-2176-0776

Complete contact information is available at: https://pubs.acs.org/10.1021/acschemneuro.3c00668

Author Contributions

M.A.J. and S.C.B. conceived this work and oversaw the experimentation. P.H., S.N., and I.J.S. carried out the experimentation in zebrafish. A.S. carried out synthesis and evaluation of the zinc photocage. P.H. and M.A.J. wrote the article. All authors have reviewed and approved the article.

Funding

This work was funded by the National Institute of Neurological Disorders and Stroke of the National Institutes of Health under Award Number R21NS109659 (M.A.J.), the National Institute of General Medical Sciences of the National Institutes of Health under Award Numbers P20GM103638 and P30GM145499, and the National Science Foundation under Award Number CHE-2004088 (S.C.B.). I.J.S. gratefully acknowledges support from the NSF REU site Grant CHE-1950293.

Notes

The authors declare no competing financial interest.

REFERENCES

- (1) Frederickson, C. J.; Suh, S. W.; Silva, D.; Frederickson, C. J.; Thompson, R. B. Importance of Zinc in the Central Nervous System: The Zinc-Containing Neuron. *J. Nutr.* **2000**, *130* (5), S1471–S1483.
- (2) Mocchegiani, E.; Bertoni-Freddari, C.; Marcellini, F.; Malavolta, M. Brain, aging and neurodegeneration: role of zinc ion availability. *Prog. Neurobiol* **2005**, *75* (6), 367–390.
- (3) Pfeiffer, C. C.; Braverman, E. R. Zinc, the brain and behavior. *Biol. Psychiatry* **1982**, *17* (4), 513–532.
- (4) Portbury, S. D.; Adlard, P. A. Zinc Signal in Brain Diseases. *Int. J. Mol. Sci.* **2017**, *18* (12), No. 2506, DOI: 10.3390/ijms18122506.
- (5) Frederickson, C. J.; Kasarskis, E. J.; Ringo, D.; Frederickson, R. E. A quinoline fluorescence method for visualizing and assaying the histochemically reactive zinc (bouton zinc) in the brain. *J. Neurosci. Methods* 1987, 20 (2), 91–103.
- (6) Frederickson, C. J. Neurobiology of zinc and zinc-containing neurons. *Int. Rev. Neurobiol.* **1989**, *31*, 145–238.
- (7) Assaf, S. Y.; Chung, S. H. Release of endogenous Zn2+ from brain tissue during activity. *Nature* **1984**, *308* (5961), 734–736.
- (8) Marger, L.; Schubert, C. R.; Bertrand, D. Zinc: An underappreciated modulatory factor of brain function. *Biochem. Pharmacol.* **2014**, 91 (4), 426–435.
- (9) Goldberg, J. M.; Lippard, S. J. Mobile zinc as a modulator of sensory perception. FEBS Lett. 2023, 597 (1), 151–165.
- (10) Howell, G. A.; Welch, M. G.; Frederickson, C. J. Stimulation-induced uptake and release of zinc in hippocampal slices. *Nature* **1984**, 308 (5961), 736–738.
- (11) Stewart, G. R.; Frederickson, C. J.; Howell, G. A.; Gage, F. H. Cholinergic denervation-induced increase of chelatable zinc in mossyfiber region of the hippocampal formation. *Brain Res.* **1984**, 290 (1), 43–51
- (12) Frederickson, C. J.; Bush, A. I. Synaptically released zinc: physiological functions and pathological effects. *BioMetals* **2001**, *14* (3–4), 353–366.
- (13) Pan, E.; Zhang, X.-a.; Huang, Z.; Krezel, A.; Zhao, M.; Tinberg, C. E.; Lippard, S. J.; McNamara, J. O. Vesicular Zinc Promotes

- Presynaptic and Inhibits Postsynaptic Long-Term Potentiation of Mossy Fiber-CA3 Synapse. *Neuron* **2011**, *71* (6), 1116–1126.
- (14) Vogt, K.; Mellor, J.; Tong, G.; Nicoll, R. The actions of synaptically released zinc at hippocampal mossy fiber synapses. *Neuron* **2000**, 26 (1), 187–196.
- (15) Gu, C.; Ewing, A. G. Simultaneous detection of vesicular content and exocytotic release with two electrodes in and at a single cell. *Chem. Sci.* **2021**, *12* (21), 7393–7400.
- (16) Pifl, C.; Wolf, A.; Rebernik, P.; Reither, H.; Berger, M. L. Zinc regulates the dopamine transporter in a membrane potential and chloride dependent manner. *Neuropharmacology* **2009**, *56* (2), 531–540.
- (17) Kalappa, B. I.; Anderson, C. T.; Goldberg, J. M.; Lippard, S. J.; Tzounopoulos, T. AMPA receptor inhibition by synaptically released zinc. *Proc. Natl. Acad. Sci. U.S.A.* **2015**, *112* (51), 15749–15754.
- (18) Jalali-Yazdi, F.; Chowdhury, S.; Yoshioka, C.; Gouaux, E. Mechanisms for Zinc and Proton Inhibition of the GluN1/GluN2A NMDA Receptor. *Cell* **2018**, *175* (6), 1520–1532.
- (19) Schulien, A. J.; Justice, J. A.; Di Maio, R.; Wills, Z. P.; Shah, N. H.; Aizenman, E. Zn(2+)-induced Ca(2+) release via ryanodine receptors triggers calcineurin-dependent redistribution of cortical neuronal Kv2.1 K(+) channels. *J. Physiol.* **2016**, *594* (10), 2647–2659.
- (20) Que, E. L.; Domaille, D. W.; Chang, C. J. Metals in Neurobiology: Probing Their Chemistry and Biology with Molecular Imaging. *Chem. Rev.* **2008**, *108* (5), 1517–1549.
- (21) Paoletti, P.; Vergnano, A. M.; Barbour, B.; Casado, M. Zinc at glutamatergic synapses. *Neuroscience* **2009**, *158* (1), 126–136.
- (22) Ellis-Davies, G. C. R. Caged compounds: photorelease technology for control of cellular chemistry and physiology. *Nat. Methods* **2007**, *4* (8), 619–628.
- (23) Ellis-Davies, G. C. R. Useful Caged Compounds for Cell Physiology. Acc. Chem. Res. 2020, 53 (8), 1593–1604.
- (24) Adams, S. R.; Tsien, R. Y. Controlling Cell Chemistry with Caged Compounds. *Annu. Rev. Physiol.* **1993**, 55 (1), 755–784.
- (25) Neher, E. Vesicle Pools and Ca 2+ Microdomains: New Tools for Understanding Their Roles in Neurotransmitter Release. *Neuron* **1998**, 20 (3), 389–399, DOI: 10.1016/s0896-6273(00)80983-6.
- (26) Ellis-Davies, G. C. R. Neurobiology with Caged Calcium. *Chem. Rev.* **2008**, *108* (5), 1603–1613.
- (27) Petersen, O. H. Ca2+ signalling and Ca2+-activated ion channels in exocrine acinar cells. *Cell Calcium* **2005**, 38 (3), 171–200.
- (28) Stocker, M. Ca2+-activated K+ channels: molecular determinants and function of the SK family. *Nat. Rev. Neurosci.* **2004**, *5* (10), 758–770.
- (29) Gomez, T. M.; Zheng, J. Q. The molecular basis for calcium-dependent axon pathfinding. *Nat. Rev. Neurosci.* **2006**, *7* (2), 115–125.
- (30) Somlyo, A. P.; Walker, J. W.; Goldman, Y. E.; Trentham, D. R.; Kobayashi, S.; Kitazawa, T.; Somlyo, A. V. Inositol trisphosphate, calcium and muscle contraction. *Philos. Trans. R. Soc. Lond. B: Biol. Sci.* 1988, 320 (1199), 399–414.
- (31) Fryer, M. W.; Zucker, R. S. Ca(2+)-dependent inactivation of Ca2+ current in Aplysia neurons: kinetic studies using photolabile Ca2+ chelators. *J. Physiol.* **1993**, *464*, 501–528.
- (32) Wang, L. Y.; Neher, E.; Taschenberger, H. Synaptic vesicles in mature calyx of Held synapses sense higher nanodomain calcium concentrations during action potential-evoked glutamate release. *J. Neurosci.* **2008**, 28 (53), 14450–14458.
- (33) Wölfel, M.; Schneggenburger, R. Presynaptic Capacitance Measurements and Ca < sup > 2</sup>⁺ Uncaging Reveal Submillisecond Exocytosis Kinetics and Characterize the Ca < sup > 2</sup>⁺ Sensitivity of Vesicle Pool Depletion at a Fast CNS Synapse. *J. Neurosci.* 2003, 23 (18), 7059–7068, DOI: 10.1523/JNEUROSCI.23-18-07059.2003.
- (34) Clapham, D. E. Calcium Signaling. *Cell* **2007**, *131* (6), 1047–1058.
- (35) Bagur, R.; Hajnóczky, G. Intracellular Ca(2+) Sensing: Its Role in Calcium Homeostasis and Signaling. *Mol. Cell* **2017**, *66* (6), 780–788.

- (36) Kawamoto, E. M.; Vivar, C.; Camandola, S. Physiology and Pathology of Calcium Signaling in the Brain. *Front. Pharmacol.* **2012**, 3, No. 61, DOI: 10.3389/fphar.2012.00061.
- (37) Basa, P. N.; Barr, C. A.; Oakley, K. M.; Liang, X.; Burdette, S. C. Zinc Photocages with Improved Photophysical Properties and Cell Permeability Imparted by Ternary Complex Formation. *J. Am. Chem. Soc.* **2019**, *141* (30), 12100–12108.
- (38) Bandara, H. M. D.; Kennedy, D. P.; Akin, E.; Incarvito, C. D.; Burdette, S. C. Photoinduced Release of Zn2+ with ZinCleav-1: a Nitrobenzyl-Based Caged Complex. *Inorg. Chem.* **2009**, *48* (17), 8445–8455
- (39) Bandara, H. M. D.; Walsh, T. P.; Burdette, S. C. A Second-Generation Photocage for Zn2+ Inspired by TPEN: Characterization and Insight into the Uncaging Quantum Yields of ZinCleav Chelators. *Chem. Eur. J.* **2011**, *17* (14), 3932–3941.
- (40) Basa, P. N.; Antala, S.; Dempski, R. E.; Burdette, S. C. A Zinc(II) Photocage Based on a Decarboxylation Metal Ion Release Mechanism for Investigating Homeostasis and Biological Signaling. *Angew. Chem., Int. Ed.* **2015**, *54* (44), 13027–13031.
- (41) Shin, M.; Field, T. M.; Stucky, C. S.; Furgurson, M. N.; Johnson, M. A. Ex Vivo Measurement of Electrically Evoked Dopamine Release in Zebrafish Whole Brain. *ACS Chem. Neurosci.* **2017**, 8 (9), 1880–1888
- (42) Venton, B. J.; Cao, Q. Fundamentals of fast-scan cyclic voltammetry for dopamine detection. *Analyst* **2020**, *145* (4), 1158–1168.
- (43) Nguyen, M. D.; Venton, B. J. Fast-scan Cyclic Voltammetry for the Characterization of Rapid Adenosine Release. *Comput. Struct. Biotechnol. J.* **2015**, *13*, 47–54.
- (44) Kaplan, S. V.; Limbocker, R. A.; Gehringer, R. C.; Divis, J. L.; Osterhaus, G. L.; Newby, M. D.; Sofis, M. J.; Jarmolowicz, D. P.; Newman, B. D.; Mathews, T. A.; Johnson, M. A. Impaired Brain Dopamine and Serotonin Release and Uptake in Wistar Rats Following Treatment with Carboplatin. ACS Chem. Neurosci. 2016, 7 (6), 689–699.
- (45) Jarosova, R.; Kaplan, S. V.; Field, T. M.; Givens, R. S.; Senadheera, S. N.; Johnson, M. A. In Situ Electrochemical Monitoring of Caged Compound Photochemistry: An Internal Actinometer for Substrate Release. *Anal. Chem.* **2021**, *93* (5), 2776–2784.
- (46) Sanford, A. L.; Morton, S. W.; Whitehouse, K. L.; Oara, H. M.; Lugo-Morales, L. Z.; Roberts, J. G.; Sombers, L. A. Voltammetric detection of hydrogen peroxide at carbon fiber microelectrodes. *Anal. Chem.* **2010**, 82 (12), 5205–5210.
- (47) Bashirzade, A. A.; Zabegalov, K. N.; Volgin, A. D.; Belova, A. S.; Demin, K. A.; de Abreu, M. S.; Babchenko, V. Y.; Bashirzade, K. A.; Yenkoyan, K. B.; Tikhonova, M. A.; Amstislavskaya, T. G.; Kalueff, A. V. Modeling neurodegenerative disorders in zebrafish. *Neurosci. Biobehav. Rev.* 2022, 138, No. 104679.
- (48) McAllister, B. B.; Dyck, R. H. A new role for zinc in the brain. *eLife* **2017**, *6*, No. e31816, DOI: 10.7554/eLife.31816.
- (49) Sanford, L.; Carpenter, M. C.; Palmer, A. E. Intracellular Zn2+transients modulate global gene expression in dissociated rat hippocampal neurons. *Sci. Rep.* **2019**, *9* (1), No. 9411.
- (50) Paoletti, P.; Ascher, P.; Neyton, J. High-Affinity Zinc Inhibition of NMDA NR1-NR2A Receptors. *J. Neurosci.* **1997**, *17* (15), 5711–5725.
- (51) Horenstein, J.; Akabas, M. H. Location of a high affinity Zn2+binding site in the channel of alpha1beta1 gamma-aminobutyric acidA receptors. *Mol. Pharmacol.* **1998**, *53* (5), 870–877.
- (52) Brautigan, D. L.; Bornstein, P.; Gallis, B. Phosphotyrosyl-protein phosphatase. Specific inhibition by Zn. *J. Biol. Chem.* **1981**, 256 (13), 6519–6522.
- (53) Li, Y.; Hasenhuetl, P. S.; Schicker, K.; Sitte, H. H.; Freissmuth, M.; Sandtner, W. Dual Action of Zn2+ on the Transport Cycle of the Dopamine Transporter. *J. Biol. Chem.* **2015**, 290 (52), 31069–31076. (54) Li, Y.; Mayer, F. P.; Hasenhuetl, P. S.; Burtscher, V.; Schicker, K.;
- Sitte, H. H.; Freissmuth, M.; Sandtner, W. Occupancy of the Zincbinding Site by Transition Metals Decreases the Substrate Affinity of

- the Human Dopamine Transporter by an Allosteric Mechanism. J. Biol. Chem. 2017, 292 (10), 4235–4243.
- (55) Stockner, T.; Montgomery, T. R.; Kudlacek, O.; Weissensteiner, R.; Ecker, G. F.; Freissmuth, M.; Sitte, H. H. Mutational analysis of the high-affinity zinc binding site validates a refined human dopamine transporter homology model. *PLoS Comput. Biol.* **2013**, 9 (2), No. e1002909.
- (56) Loland, C. J.; Norregaard, L.; Gether, U. Defining proximity relationships in the tertiary structure of the dopamine transporter. Identification of a conserved glutamic acid as a third coordinate in the endogenous Zn(2+)-binding site. *J. Biol. Chem.* **1999**, 274 (52), 36928–36934.
- (57) Norregaard, L.; Frederiksen, D.; Nielsen, E. O.; Gether, U. Delineation of an endogenous zinc-binding site in the human dopamine transporter. *EMBO J.* **1998**, *17* (15), 4266–4273.
- (58) Pifl, C.; Rebernik, P.; Kattinger, A.; Reither, H. Zn2+ modulates currents generated by the dopamine transporter: parallel effects on amphetamine-induced charge transfer and release. *Neuropharmacology* **2004**, *46* (2), 223–231.
- (59) Turner, T. Y.; Soliman, M. R. I. Effects of zinc on spatial reference memory and brain dopamine (D1) receptor binding kinetics in rats. *Prog. Neuro-Psychopharmacol. Biol. Psychiatry* **2000**, 24 (7), 1203–1217.
- (60) Schetz, J. A.; Sibley, D. R. Zinc allosterically modulates antagonist binding to cloned D1 and D2 dopamine receptors. *J. Neurochem.* **1997**, 68 (5), 1990–1997.
- (61) Herlitze, S.; Garcia, D. E.; Mackie, K.; Hille, B.; Scheuer, T.; Catterall, W. A. Modulation of Ca2+ channels by G-protein beta gamma subunits. *Nature* **1996**, 380 (6571), 258–262.
- (62) Ikeda, S. R. Voltage-dependent modulation of N-type calcium channels by G-protein beta gamma subunits. *Nature* **1996**, 380 (6571), 255–258
- (63) Fulton, S.; Thibault, D.; Mendez, J. A.; Lahaie, N.; Tirotta, E.; Borrelli, E.; Bouvier, M.; Tempel, B. L.; Trudeau, L. E. Contribution of Kv1.2 voltage-gated potassium channel to D2 autoreceptor regulation of axonal dopamine overflow. *J. Biol. Chem.* **2011**, 286 (11), 9360–9372
- (64) Martel, P.; Leo, D.; Fulton, S.; Berard, M.; Trudeau, L. E. Role of Kv1 potassium channels in regulating dopamine release and presynaptic D2 receptor function. *PLoS One* **2011**, *6* (5), No. e20402.
- (65) Benoit-Marand, M.; Ballion, B.; Borrelli, E.; Boraud, T.; Gonon, F. Inhibition of dopamine uptake by D2 antagonists: an in vivo study. *J. Neurochem.* **2011**, *116* (3), 449–458.
- (66) Cass, W. A.; Gerhardt, G. A. Direct in vivo evidence that D2 dopamine receptors can modulate dopamine uptake. *Neurosci. Lett.* **1994**, 176 (2), 259–263.
- (67) Dickinson, S. D.; Sabeti, J.; Larson, G. A.; Giardina, K.; Rubinstein, M.; Kelly, M. A.; Grandy, D. K.; Low, M. J.; Gerhardt, G. A.; Zahniser, N. R. Dopamine D2 receptor-deficient mice exhibit decreased dopamine transporter function but no changes in dopamine release in dorsal striatum. *J. Neurochem.* **1999**, 72 (1), 148–156.
- (68) Mayfield, R. D.; Zahniser, N. R. Dopamine D2 receptor regulation of the dopamine transporter expressed in Xenopus laevis oocytes is voltage-independent. *Mol. Pharmacol.* **2001**, 59 (1), 113–121.
- (69) Schmitz, Y.; Benoit-Marand, M.; Gonon, F.; Sulzer, D. Presynaptic regulation of dopaminergic neurotransmission. *J. Neurochem.* **2003**, 87 (2), 273–289.
- (70) Wu, L. G.; Saggau, P. Presynaptic inhibition of elicited neurotransmitter release. *Trends Neurosci.* **1997**, 20 (5), 204–212.
- (71) Phillips, P. E.; Hancock, P. J.; Stamford, J. A. Time window of autoreceptor-mediated inhibition of limbic and striatal dopamine release. *Synapse* **2002**, *44* (1), 15–22.
- (72) Kehr, W.; Carlsson, A.; Lindqvist, M.; Magnusson, T.; Atack, C. Evidence for a receptor-mediated feedback control of striatal tyrosine hydroxylase activity. *J. Pharm. Pharmacol.* **2011**, 24 (9), 744–747.
- (73) Wolf, M. E.; Roth, R. H. Autoreceptor regulation of dopamine synthesis. *Ann. N. Y. Acad. Sci.* **1990**, *604*, 323–343.

- (74) Hettiarachchi, P.; Johnson, M. A. Characterization of D3 Autoreceptor Function in Whole Zebrafish Brain with Fast-Scan Cyclic Voltammetry. ACS Chem. Neurosci. 2022, 13 (19), 2863–2873.
- (75) Manzerra, P.; Behrens, M. M.; Canzoniero, L. M.; Wang, X. Q.; Heidinger, V.; Ichinose, T.; Yu, S. P.; Choi, D. W. Zinc induces a Src family kinase-mediated up-regulation of NMDA receptor activity and excitotoxicity. *Proc. Natl. Acad. Sci. U.S.A.* **2001**, 98 (20), 11055–11061.
- (76) Huang, Y. Z.; McNamara, J. O. Mutual regulation of Src family kinases and the neurotrophin receptor TrkB. *J. Biol. Chem.* **2010**, 285 (11), 8207–8217.
- (77) Kimura, T.; Kambe, T. The Functions of Metallothionein and ZIP and ZnT Transporters: An Overview and Perspective. *Int. J. Mol. Sci.* **2016**, *17* (3), 336.
- (78) Palmiter, R. D. Protection against zinc toxicity by metallothionein and zinc transporter 1. *Proc. Natl. Acad. Sci. U.S.A.* **2004**, *101* (14), 4918–4923.
- (79) Gao, H.; Boillat, A.; Huang, D.; Liang, C.; Peers, C.; Gamper, N. Intracellular zinc activates KCNQ channels by reducing their dependence on phosphatidylinositol 4,5-bisphosphate. *Proc. Natl. Acad. Sci. U.S.A.* **2017**, *114* (31), E6410–E6419.
- (80) Syková, E.; Nicholson, C. Diffusion in brain extracellular space. *Physiol. Rev.* **2008**, 88 (4), 1277–1340.
- (81) Wolf, C.; Weth, A.; Walcher, S.; Lax, C.; Baumgartner, W. Modeling of Zinc Dynamics in the Synaptic Cleft: Implications for Cadherin Mediated Adhesion and Synaptic Plasticity. *Front. Mol. Neurosci.* **2018**, *11*, No. 306, DOI: 10.3389/fnmol.2018.00306.
- (82) Maret, W. The function of zinc metallothionein: a link between cellular zinc and redox state. *J. Nutr.* **2000**, *130* (5S Suppl), 1455S–1458S.
- (83) Kambe, T.; Taylor, K. M.; Fu, D. Zinc transporters and their functional integration in mammalian cells. *J. Biol. Chem.* **2021**, 296, No. 100320.
- (84) Wang, B.; Fang, T.; Chen, H. Zinc and Central Nervous System Disorders. *Nutrients* **2023**, *15* (9), No. 2140, DOI: 10.3390/nu15092140.
- (85) Ji, J. A.; Zhang, B.; Cheng, W.; Wang, Y. J. Methionine, tryptophan, and histidine oxidation in a model protein, PTH: mechanisms and stabilization. *J. Pharm. Sci.* **2009**, *98* (12), 4485–4500.
- (86) Joshi, A. Selective Serotonin Re-uptake Inhibitors: An overview. *Psychiatr. Danub.* **2018**, *30* (Suppl 7), 605–609.
- (87) Satała, G.; Duszynska, B.; Stachowicz, K.; Rafalo, A.; Pochwat, B.; Luckhart, C.; Albert, P. R.; Daigle, M.; Tanaka, K. F.; Hen, R.; Lenda, T.; Nowak, G.; Bojarski, A. J.; Szewczyk, B. Concentration-Dependent Dual Mode of Zn Action at Serotonin 5-HT1A Receptors: In Vitro and In Vivo Studies. *Mol. Neurobiol.* **2016**, *53* (10), 6869–6881.
- (88) Watt, N. T.; Whitehouse, I. J.; Hooper, N. M. The role of zinc in Alzheimer's disease. *Int. J. Alzheimers Dis.* **2010**, 2011, No. 971021, DOI: 10.4061/2011/971021.
- (89) Sikora, J.; Ouagazzal, A. M. Synaptic Zinc: An Emerging Player in Parkinson's Disease. *Int. J. Mol. Sci.* **2021**, 22 (9), No. 4724, DOI: 10.3390/ijms22094724.
- (90) da Silva, H. F. L.; Brito, A. N. A.; Freitas, E. P. S.; Dourado, M. E. T., Jr.; Sena-Evangelista, K. C. M.; Lais, L. L. Dietary intake and zinc status in amyotrophic lateral sclerosis patients. *Nutr. Hosp.* **2017**, *34* (5), 1361–1367, DOI: 10.20960/nh.1004.
- (91) Cope, E. C.; Morris, D. R.; Levenson, C. W. Improving treatments and outcomes: an emerging role for zinc in traumatic brain injury. *Nutr. Rev.* **2012**, *70* (7), 410–413.
- (92) Petrilli, M. A.; Kranz, T. M.; Kleinhaus, K.; Joe, P.; Getz, M.; Johnson, P.; Chao, M. V.; Malaspina, D. The Emerging Role for Zinc in Depression and Psychosis. *Front. Pharmacol.* **2017**, *8*, 414.
- (93) Joe, P.; Petrilli, M.; Malaspina, D.; Weissman, J. Zinc in schizophrenia: A meta-analysis. *Gen. Hosp. Psychiatry* **2018**, 53, 19–24. (94) Shigemoto, A. K.; Bhattacharjee, A.; Hickey, E. E.; Boyd, H. J.; McCormick, T. M.; Burdette, S. C. Improved Photodecarboxylation Properties in Zinc Photocages Constructed Using m-Nitrophenylacetic Acid Variants. *ChemPhotoChem* **2022**, 6 (9), No. e202200102.

(95) Mao, L.; Jin, J.; Song, L.-n.; Yamamoto, K.; Jin, L. Electrochemical Microsensor for In Vivo Measurements of Oxygen Based on Nafion and Methylviologen Modified Carbon Fiber Microelectrode. *Electroanalysis* 1999, 11 (7), 499–504.